



Review

Cyclometallated iridium complexes for conversion of light into electricity and electricity into light

Etienne Baranoff, Jun-Ho Yum, Michael Graetzel, Md.K. Nazeeruddin *

Institute of Chemical Sciences and Engineering, School of Basic Sciences, Swiss Federal Institute of Technology, CH-1015 Lausanne, Switzerland

ARTICLE INFO

Article history:

Received 30 January 2009
 Received in revised form 25 February 2009
 Accepted 26 February 2009
 Available online 10 March 2009

Keywords:

Cyclometallated iridium complexes
 Organic light-emitting devices
 Dye-sensitized solar cells
 Organometallic complexes
 Triplet emitters
 Sensitizers

ABSTRACT

This brief review describes applications of cyclometallated iridium complexes for energy saving organic light-emitting devices (OLED's) and energy generating molecular photovoltaic cells. The first part consists of a short overview of the methods to modulate emitted color and quantum yield in neutral and ionic complexes for light-emitting diodes. And in the second part, we report initial results of cyclometallated iridium complexes for solar cell applications.

© 2009 Elsevier B.V. All rights reserved.

Contents

1. Introduction	2661
2. Cyclometallated iridium complexes for OLED applications	2662
2.1. General photophysical properties	2662
2.2. Neutral tris-cyclometallated iridium complexes	2662
2.3. Neutral bis-cyclometallated iridium complexes	2665
2.4. Anionic bis-cyclometallated iridium complexes	2666
2.5. Cationic bis-cyclometallated iridium complexes	2666
2.6. Controlling the phosphorescence quantum yield	2667
2.7. Sublimation not an innocent technique	2667
3. Iridium complexes for DSSC	2667
4. Future prospects	2669
Acknowledgements	2670
References	2670

1. Introduction

Climatologist are pointing to global warming threatening our planet and some fossils fuels like oil are coming close to their overall production peak. Therefore, in a political shift for a sustainable world, developed and developing countries are taking actions on energy issues, aiming for a reduction of worldwide energy consumption and increase of the production of energy originating from renewable sources.

Lighting applications account for about 19% of the electricity consumption of the world, therefore low energy consumption devices such as organic light-emitting devices (OLEDs), have been considered as the most promising solution for decreasing overall energy consumption. In this respect iridium(III) cyclometallated complexes are attracting wide spread interest because of their unique photophysical properties [1]. In order to solve the second target, it is important to note that the obvious main energy source for renewable energy is coming from the sun. In that respect, dye-sensitized solar cells (DSSC) are considered as being the most promising solution for harnessing the energy of the sun and converting it into electrical energy. Using ruthenium complexes 11% power

* Corresponding author. Tel.: +41 21 693 6124; fax: +41 21 693 4111.
 E-mail address: mdkhaja.nazeeruddin@epfl.ch (Md.K. Nazeeruddin).

conversion efficiency under AM1.5 conditions have been obtained [2]. In dye-sensitized solar cells ruthenium has without any doubt the lion share of the studied dyes [3]. However, recently other metal complexes as well as metal-free organic dyes are testing the supremacy of ruthenium [4]. Iridium complexes are far from competing with ruthenium, however iridium complexes exhibited some interesting behavior worthwhile having a closer look at them [5]. We will shortly review the iridium complexes, which are useful in energy saving (light-emitting diodes) and energy generating (dye-sensitized solar cells) applications.

2. Cyclometallated iridium complexes for OLED applications

The last decade witnessed an explosion of the number of reported luminescent cyclometallated iridium(III) complexes. This widespread interest originates from their wide color tunability and high phosphorescence quantum yield, which make them very attractive for application in organic light-emitting diodes (OLEDs). Neutral iridium cyclometallated complexes have been used extensively in OLEDs and obtained up to 19% external quantum efficiencies, using multilayered structure for charge injection, transport, and light emission [6]. This long standing record has been broken recently with devices exhibiting more than 20% external quantum efficiencies. They rely on the use of newly developed host materials with improved charge transporting capabilities [7].

Simplified working principle of OLED is shown in Fig. 1. A layer of emissive material is sandwiched between a cathode and an anode. When the device is biased, holes are injected in the HOMO level of the material and electron are injected in the LUMO level. Both electron and hole will be transported to the other electrode. If a hole and an electron are passing close enough from each other, they may interact and finally recombine to lead to an exciton, which will deactivate by emitting light. In order to improve injection and transporting properties in the device, multilayer architectures are usually used.

2.1. General photophysical properties

In metal complexes there are three types of excited states: (a) metal-centered (MC) excited states, from the promotion of an electron from t_{2g} to e_g orbitals; (b) ligand-centered (LC) states that are $\pi-\pi^*$ transitions; (c) metal-to-ligand charge transfer states (MLCT), which can be understood with the aid of an energy level diagram shown in Fig. 2. Singlet-singlet absorptions are an electronic transition from metal t_{2g} orbitals to empty ligand orbitals or centered on the ligand, that is from π orbitals to empty π^* orbitals, without spin change, which are allowed and are identified by large extinction coefficients. On the contrary, singlet-triplet absorptions are transitions with spin change and are forbidden, therefore associated with small extinction coefficients. However, a singlet state may be involved in spin flip, which is called intersystem crossing

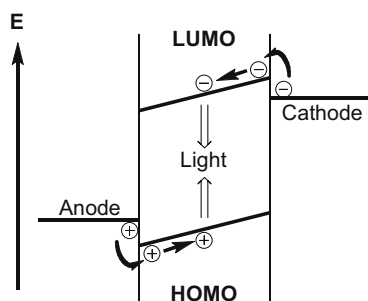


Fig. 1. Operating principles of OLED.

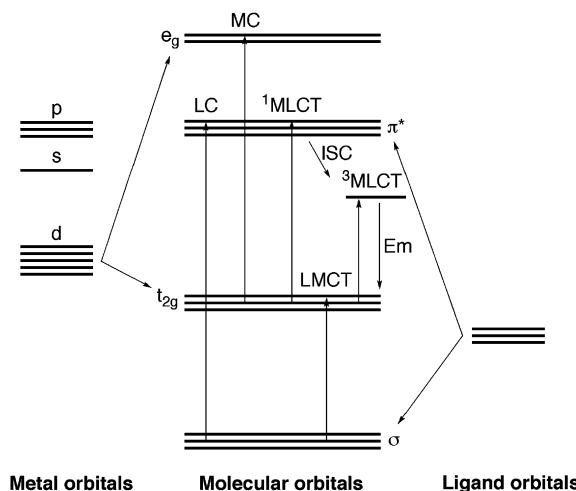
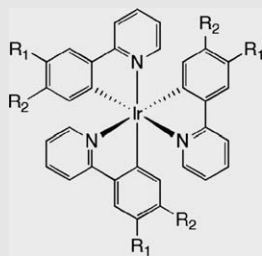


Fig. 2. Schematic and simplified molecular orbital diagram for an octahedral d^6 metal complex involving 2-phenylpyridine (C_3 symmetry)-type ligands in which various possible transitions are indicated.

(ISC), resulting in an excited triplet state. The radiative process of a singlet and triplet excited states to a singlet ground state are termed fluorescence and phosphorescence, respectively. In cyclometallated iridium complexes, the excited triplet state, which is responsible for phosphorescence, is a combination of the LC and the MLCT triplet excited state, that is a mixed (triplet) excited state. As iridium complexes possess strong spin-orbit coupling, excited singlet states can undergo efficient ISC into the triplet state resulting in high phosphorescence quantum yields. However, not all the complexes are highly luminescent because of the different deactivation pathways. The choice of iridium metal is of special interest for a number of reasons: (a) because of its quasi-octahedral geometry one can introduce specific ligands in a controlled manner; (b) the photophysical and the electrochemical properties of iridium complexes can be tuned in a predictable way; (c) the iridium metal possess stable and accessible oxidation and reduction states; and (d) cyclometallated iridium complexes are known to have highest triplet quantum yields.

2.2. Neutral tris-cyclometallated iridium complexes

Tris-cyclometallated iridium complexes are neutral complexes of the type $Ir(C^{\wedge}N)_3$. The archetype of such complexes is $Ir(ppy)_3$ ($ppy = 2$ -phenylpyridine), where the coordination of ppy ligand to metal is analogous to that found in 2,2'-bipyridine except that one nitrogen is replaced by carbon anion. The absorption spectra of $[Ir(ppy)_3]$ display strong ligand-to-ligand (LC, $\pi-\pi^*$) and MLCT transitions in the UV and the visible region, respectively. The MLCT transition bands are lower in energy than the LC $\pi-\pi^*$ transitions. The excited triplet state shows strong phosphorescence in the green region at around 515 nm, with an excited state lifetime of 2 μs [8]. Since the analysis of the spectral properties of $Ir(ppy)_3$ complex using DFT by Hay, it is known that the HOMO in tris-phenylpyridine $Ir(III)$ $[Ir(ppy)_3]$ is principally composed of π orbitals of the phenyl ring and the metal d -orbitals. The pyridine is formally neutral and is the major contributor to the LUMO in the $[Ir(ppy)_3]$ complex [9]. In a practical approximation, the emission maximum of luminescent iridium complexes is determined principally by the HOMO-LUMO gap. An effective strategy to tune the emission color in $Ir(III)$ complexes relies on the selective stabilization or destabilization of the HOMO and/or LUMO of the complex. Watts et al. synthesized several substituted ppy -based neutral iridium complexes (Table 1) [8,10].

Table 1
Emission, lifetime and electrochemical data of complexes 1–8.


1 : R₁=H ; R₂=H
 2 : R₁=H ; R₂=CH₃
 3 : R₁=H ; R₂=C₃H₇
 4 : R₁=H ; R₂=*t*Bu
 5 : R₁=H ; R₂=F
 6 : R₁=H ; R₂=CF₃
 7 : R₁=H ; R₂=OCH₃
 8 : R₁=OCH₃ ; R₂=H

Complex	Emission λ_{\max}^a (nm)	Lifetime τ^b (μ s)	Potential vs. Fc ^{+/0} $E_{1/2ox}$ (V)	Hammett constant σ [11]
1	494	1.9	0.37	0.00
2	493	1.9	0.30	-0.07
3	496	1.9	0.27	-0.06
4	497	2.0	0.26	-0.10
5	468	2.0	0.57	0.34
6	494	2.2	0.68	0.43
7	481	2.2	0.35	0.12
8	539	2.9	0.15	-0.27

^a Shortest wavelength feature in emission spectrum in ethanol/methanol glass (1:1 by volume) at 77 K.

^b Emission lifetime in degassed acetonitrile at room temperature.

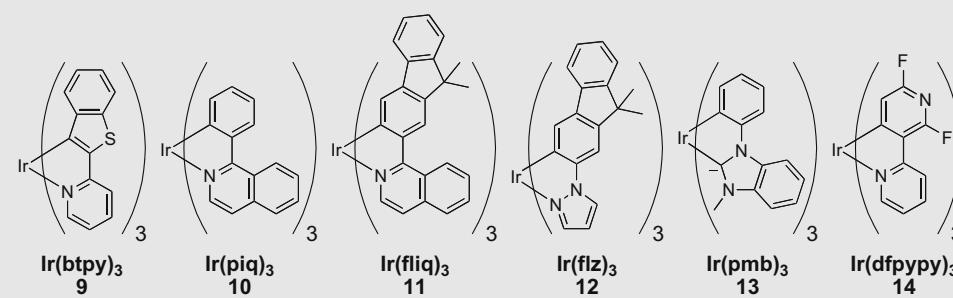
The photophysical and electrochemical data (see Table 1) demonstrate the influence of ligands bearing electron-withdrawing and electron-donating substituents. It is interesting to note the difference between complexes 7 and 8, which is simply the effect of the position of electron-donating substitution on the phenyl ring. In complex 8 the electron-donating group is substituted at the three-position of the phenyl ring. This destabilizes the HOMO by 0.2 V as compared to complex 7 in which the electron-donating group is substituted at four-position. This can be rationalized when one look at the Hammett substituent constant for the substituent depending on its position relative to the carbon coordinated to the iridium center. When in the meta position (complex 7) the methoxy group is an acceptor group ($\sigma = 0.12$) due to an inductive

effect, whereas in the para position (complex 8) the methoxy group is a donor group ($\sigma = -0.27$), due to a mesomeric effect (oxygen lone pair donation to the aromatic π orbitals). From the electrochemical data of the complexes shown in Table 1, it is evident that the less positive oxidation potential values result from ligands with electron-donating substituents, and more positive oxidation potential values result from ligands with electron-withdrawing substituents. In other words, electron-withdrawing substituents on the phenyl of the C[^]N ligands decrease the donation to the metal and therefore stabilize the metal-based HOMO. Electron-releasing substituents on the phenyl of the C[^]N ligand lead, on the other hand, to destabilization of the HOMO. When substituents are on the pyridine rings, effect will mostly be a stabilization of the LUMO for electron-acceptor groups and destabilization for electron-donor groups.

Another tool for adjusting the HOMO–LUMO levels, is to replace the phenyl or the pyridine in the C[^]N ligand by other groups (Table 2). For example, benzothienyl, quinoline, fluorene, triarylamine or carbazole groups have been used for developing new red emitting complexes [12]. This approach relies on the extension of the aromatic delocalization for stabilizing the LUMO or destabilizing the HOMO, leading to a reduced HOMO–LUMO gap. Reducing the aromatic delocalization in an attempt to blue shift the emission, using for example a vinyl group in place of the phenyl, failed [13]. To achieve a blue shift of the emission, replacing the pyridine with moieties that destabilize the LUMO level relatively to the HOMO level of the phenyl has been achieved using pyrazolyl and carbenes group [14]. It is also possible to stabilize even more the HOMO level of the complex by replacing the phenyl with a pyridine, which coordinates through the carbon in para position of the nitrogen [15].

An interesting feature of tris-cyclometallated iridium complexes is that they can have either a facial (*fac*) or a meridional (*mer*) configuration. It has been shown by Thompson et al., that such isomers have pronounced differences in their photophysical properties (Table 3) as red-shifted emission and decreased quantum efficiencies have been observed for the meridional isomers relative to their facial analogues [16].

It is possible to convert the meridional isomers to the facial one using either thermal or photochemical routes, indicating that the

Table 2
Photophysical properties of complexes 9–14.


Complex	Emission λ_{\max} (nm)	Φ_p	Lifetime τ (μ s)
9 Ir(btpy) ₃ ^a	596	0.12	4.0
10 Ir(piQ) ₃ ^a	620	0.26	0.74
11 Ir(fliQ) ₃ ^a	652	0.19	0.74
12 Ir(flz) ₃ ^b	480	0.38	37
13 Ir(pmb) ₃ ^b	380	0.04	0.22
14 Ir(dfppy) ₃ ^c	438	0.71	–

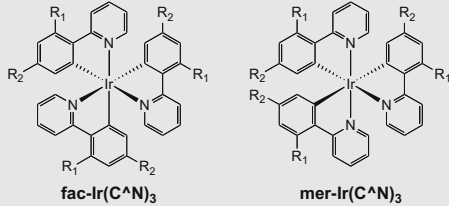
Ligand abbreviation: btpy = 2-(benzo[*b*]thiophen-2-yl)bipyridine; piQ = 1-phenylisoquinoline; fliQ = 1-(9,9-dimethyl-9H-fluoren-2-yl)isoquinoline; flz = 1-[(9,9-dimethyl-2-fluorenyl)]pyrazole; pmb = 1-phenyl-3-methyl benzimidazole; dfppy = 2,6-difluoro-2,3-bipyridine.

^a Deaerated toluene solution at 298 K.

^b Deaerated 2-MeTHF solution at room temperature.

^c Deaerated CH₂Cl₂ at room temperature.

Table 3
Properties of selected *fac* and *mer* isomers.



15 : R₁=H ; R₂=H
16 : R₁=H ; R₂=CH₃
17 : R₁=F ; R₂=F

Ligand C ^N	Isomer	Emission at 77 K λ_{\max}^a (nm)	Lifetime at 77 K τ^a (μ s)	Emission at 298 K λ_{\max} (nm)	Lifetime at 298 K τ (μ s)	Potential vs. Fc ^{c+/0} E _{1/2ox} ^b (V)	Potential vs. Fc ^{c+/0} E _{1/2red} ^b (V)
15	<i>fac</i>	492	3.6	510	1.9	0.31	-2.70
	<i>mer</i>	493	4.2	512	0.15	0.25	-2.63
16	<i>fac</i>	492	3.0	510	2.0	0.30	-2.78
	<i>mer</i>	530	4.8	550	0.26	0.18	-2.73
17	<i>fac</i>	450	2.5	468	1.6	0.78	-2.51
	<i>mer</i>	460	5.4	482	0.21	0.69	-2.50

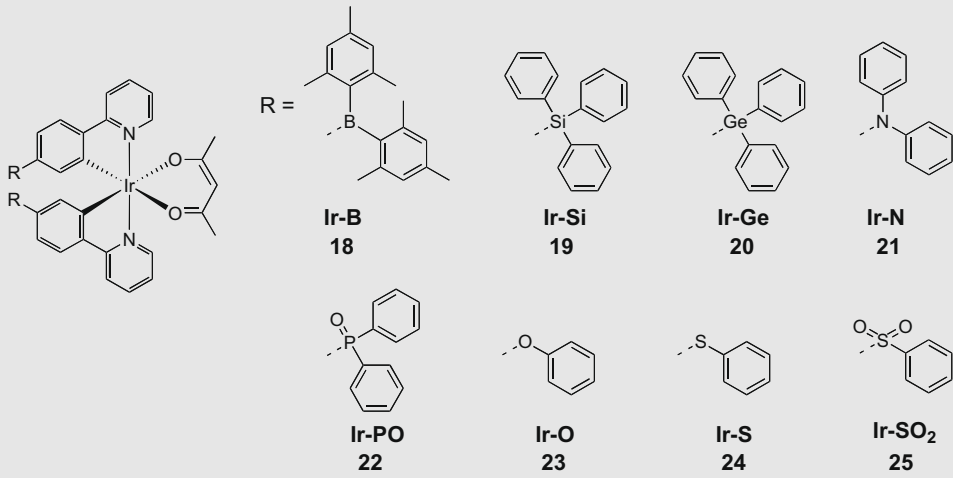
^a In 2-MeTHF.

^b In DMF.

facial isomers is thermodynamically more stable than the meridional analogue. On the other hand, in the case of Ir(C^{C:})₃ complexes, that is complexes containing a carbene moiety, isomerization could not be achieved either thermally or photochemically, and degradation of the compound is observed. This failure is presumed to come from the stronger Ir–C_{carbene} bond than Ir–N_{pyridine} bond making the dissociation of the ligand needed for isomerization more difficult for the Ir(C^{C:})₃ complexes. Interest-

ingly, having pure samples of non-interconvertible facial and meridional isomers gives the opportunity to prepare OLEDs using either the facial isomer or the meridional isomer as the phosphorescent dopant [17]. This has been done using Ir(pmb)₃ complex. It is surprising that while the *fac*-Ir(pmb)₃ complex has a photoluminescence quantum yield roughly one order of magnitude higher than the *mer*-Ir(pmb)₃ complex in solution, OLEDs prepared with *mer*-Ir(pmb)₃ have efficiencies about twice higher than those pre-

Table 4
Photophysical and electrochemical properties of complexes **18–25**.



Complex	Emission ^a λ_{\max} at 293 K (nm)	Quantum yield ^d Φ_p	Lifetime ^a τ (μ s)	Potential ^b E _{1/2ox} (V)	Potential ^b E _{1/2red} (V)
18	605	0.18	2.67	0.36	-2.41 -2.63 -2.88
19	535	0.39	2.44	0.38	-2.69
20	530	0.40	2.17	0.42	-2.72
21	533	0.14	5.00	0.31	-2.82
22	541	0.19	2.56	0.58	-2.40 -2.64
23	505	0.40	1.66	0.42	-2.80
24	527	0.52	4.87	0.41	-2.72
25	550	0.86	3.13	0.66, 0.83	-2.26 -2.48

^a In degassed toluene solution.

^b In THF solution.

Table 5
Photophysical and electrochemical properties of complexes **26–29**.

Complex	Emission ^a λ_{max} at RT (nm)	Quantum yield ^a Φ_p	Lifetime ^a τ (μs)	Potential vs. $\text{Fc}^{+/0b}$	
				$E_{1/2\text{ox}}$ (V)	$E_{1/2\text{red}}$ (V)
26	437, 460	0.10	0.10	1.00	–2.55
27	464, 488	0.45	2.77	0.85	–2.74
28	456, 480	0.20	1.23	0.83	–3.11
29	434, 457	0.04	0.07	1.09	–2.53

^a In degassed dichloromethane solution.^b In dichloromethane and THF solutions.

pared with *fac*-Ir(pmb)₃. This result is said to come from the different HOMO and triplet energies of the two species.

2.3. Neutral bis-cyclometallated iridium complexes

Mixed ligand Ir complexes with C^N cyclometallating ligands, are particularly appealing for tuning the photophysical properties of the complexes, since the two types of ligands, the main cyclometallated ligand and the ancillary ligand, can be almost independently functionalized to obtain the desired color tuning [18].

Overall there is no difference in tuning strategies between tris-cyclometallated complexes and bis-cyclometallated complexes when the main cyclometallating ligand is involved. The main advantage of bis-cyclometallated complexes compared to the tris-cyclometallated family, is the synthesis requiring less harsh conditions. Consequences are higher yields and no issue with isomers as shown in Section 2.2. A recent report about color tuning based on modification of the main ligand is worth noting [19]. The series of complexes studied is based on Ir(ppy)₂(acac) with substituents on the four-position of the phenyl and is named **Ir-N** (Table 4).

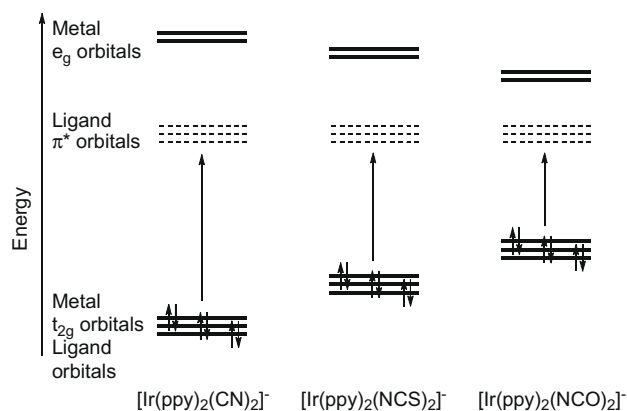
Table 6
Photophysical properties of complexes **30–35**.

Complex	Emission (nm)	HOMO (eV)	Φ_p	ΔE_{LUMO} (eV)
30	468	5.8	0.42	0.000
31	478	5.9	0.31	0.000
32	573	5.9	0.35	–0.048
33	581	5.8	0.27	–0.196
34	587	5.9	0.31	–0.466
35	666	5.8	0.39	–0.801

The complexes **Ir-N** exhibit fair to high photoluminescence quantum yield in toluene solution. In addition, the lifetimes of the excited state are in the microseconds range, which is expected from phosphorescent cyclometallated iridium complexes. The emitted color varies from bluish-green for **23** to orange-red for **18**. Interestingly, the color is not directly tuned due to the acceptor/donor properties of the substituents. Indeed, the complexes **22**, **25**, and **18**, where the substituents are electron-withdrawing groups, show bathochromic shifts in their emission maxima relative to the parent Ir(ppy)₂(acac) complex. Such effect was already observed for example when trifluoromethane groups are used [20].

Another approach to tune the emitted color, particularly suitable for blue-emitting complexes, rely on the breaking of the conjugation in the cyclometallating main ligand [21]. The introduction of the methylene bridge in complexes **26–29**, Table 5, stabilizes the π orbitals and destabilizes the π^* orbitals of the ligand. As a result the LUMO orbital of the complexes is located on the pyridyl azolate ligand, and in the case of complex **27**, the HOMO as well is located on the ancillary ligand. In commonly used conjugated cyclometallating ligand, substitution on one part of the ligand usually induces adverse effects on the other part. This results in only small gains if one wants to blueshift the emission of a complex. In the case of non-conjugated ligands, each part can be substituted independently as the communication between both sides of the ligand is broken by the –CH₂– bridge.

The complexes **26–29** can be understood as an application of the color tuning strategy developed by Park et al. using the ancil-

**Fig. 3.** Schematic drawing of HOMO and LUMO orbitals for complexes **36–38**.

lary ligand. They have demonstrated that a broad range of color tuning can be achieved by controlling the energy level of the ancillary ligand relative to the LUMO level of the main ligand [22]. By using ancillary ligand with different band gap energy, while keeping the cyclometallating ligand unchanged, emission color ranging from sky blue to red could be observed. The mechanism is said to come from efficient inter-ligand energy transfer (ILET) to the “emitting ancillary ligand”, after excitation from the iridium-centered HOMO to the cyclometallating difluorophenylpyridine-centered LUMO. If considered unchanged HOMO levels within this family of complexes, the more negative is ΔE_{LUMO} , that is the lower the LUMO of the ancillary ligand compared to the LUMO of the main ligand, the smaller the HOMO–LUMO gap, that is the stronger the red-shift observed (Table 6).

2.4. Anionic bis-cyclometallated iridium complexes

Color tuning can be achieved by tuning the HOMO energy level in Ir pseudohalogen complexes of the type $\text{TBA}[\text{Ir}(\text{ppy})_2(\text{CN})_2]$ (**36**), $\text{TBA}[\text{Ir}(\text{ppy})_2(\text{NCS})_2]$ (**37**), and $\text{TBA}[\text{Ir}(\text{ppy})_2(\text{NCO})_2]$ (**38**) as shown in Fig. 3 [6d].

The cyclic voltammograms of **36**, **37**, and **38** show a quasi-reversible oxidation potential at 0.91, 0.45, and 0.18 V vs. ferrocene–ferrocene, respectively. Changes in the electron-donating or electron-withdrawing nature of the ancillary ligands can result in a variation of electronic properties at the metal center. It is interesting to compare these three complexes that contain cyanide, thiocyanate, and isocyanate ligands. The 0.73 V anodic shift in oxidation potential of **36** compared to complex **38** shows the extent of π back-bonding to the cyanide ligand from the Ir(III) center. The enormous enhancement in π back-bonding leads to significant blue shift of the emission maxima of complex **36** compared to complexes **37** and **38**.

The absorption spectra of these complexes display bands in the UV and the visible region due to intraligand (π – π^*) and MLCT transitions, respectively [23]. The MLCT band in **36** (463 nm) is significantly blue-shifted compared to **37** (478 nm), and **38** (494 nm), indicating the extent of π -acceptor strength of the CN^- ligand com-

pared to the NCS^- and NCO^- ligands. The spectral shifts are consistent with the electrochemical data of these complexes.

2.5. Cationic bis-cyclometallated iridium complexes

The tuning aspect of the MLCT transitions in cationic Ir complexes is illustrated by considering the following complexes: $[\text{Ir}(\text{2-phenylpyridine})_2(4,4'\text{-tert-butyl-2,2'-bipyridine})]\text{PF}_6$ (**39**), $[\text{Ir}(\text{2,4-difluorophenylpyridine})_2(4,4'\text{-dimethylamino-2,2'-bipyridine})]\text{PF}_6$ (**40**), and $[\text{Ir}(\text{2-phenylpyridine})_2(4,4'\text{-dimethylamino-2,2'-bipyridine})]\text{PF}_6$ (**41**). The cyclic voltammogram of complex **41** shows a reversible wave at 0.72 V vs. $\text{Fc}^{+/0}$ due to oxidation of Ir(III)–Ir(IV), which is cathodically shifted by 210 mV compared to complex **39** due to the donor strength of 4,4'-dimethylamino-2,2'-bipyridine [24]. The three reversible reduction waves at –2.17 and –2.61 and –2.87 V vs. $\text{Fc}^{+/0}$ are assigned to the reduction of 4,4'-dimethylamino-2,2'-bipyridine and the two ppy ligands, respectively. It is interesting to note that the ligand-based reduction potential of **41** is significantly shifted cathodically (390 mV) compared to complex **39**, demonstrating that the destabilization of the LUMO orbitals of 4,4'-dimethylamino-2,2'-bipyridine, which offsets more than the destabilization of the Ir HOMO orbitals caused by the electron-donating 4,4'-dimethylamino-2,2'-bipyridine ligand, ensuing an increase in the gap between the HOMO and the LUMO of **41** compared to the HOMO–LUMO gap of complex **39**.

The cyclic voltammogram of complex **40** shows a reversible couple at 1.0 V vs. $\text{Fc}^{+/0}$ due to oxidation of Ir(III)–Ir(IV), and two reversible reduction waves at –2.13 and –2.49 V vs. $\text{Fc}^{+/0}$ arising from the reduction of the 4,4'-dimethylamino-2,2'-bipyridine and 2-(2,4-difluorophenyl)pyridine ligand, respectively. The HOMO orbitals in **40** are stabilized upon insertion of fluoro substituents on the ppy ligands, thus ensuing an increase of the HOMO and LUMO gap of **40** compared to the HOMO and LUMO gap of **39** and **41** (Table 7) [24b].

UV–vis absorption spectra of the complexes **39**, **40**, and **41** in dichloromethane solution at 298 K display bands in the UV and the visible region due to intraligand (π – π^*) and MLCT transitions,

Table 7
Photophysical and electrochemical properties of complexes **39**–**41**.

Complex	Absorption ^a λ_{max} (nm)	Emission ^b λ_{max} (nm)	Potential ^c vs. $\text{Fc}^{+/0}$		Lifetime ^d τ (μs)
			$E_{1/2\text{ox}}$ (V)	$E_{1/2\text{red}}$ (V)	
39	–	581 ^e	0.88 ^e	–1.83 ^e	0.557 ^e
40	266 (8.27), 316 (2.89), 344 (2.20), 376 (1.45), 410 (0.41), 444 (0.14)	463, 493	1.0	–2.13	4.11
				–2.49	
41	268 (5.62), 290 (3.49), 356 (0.95), 376 (0.85), 444 (0.19)	491, 520	0.75	–2.77	2.43
				–2.17	
				–2.61	
				–2.87	

^a Absorption data were measured in CH_2Cl_2 solution. Brackets contain values for molar extinction coefficient (ϵ) in $10^4 \text{ M}^{-1} \text{ cm}^{-1}$.

^b Emission data were collected at 298 K by exciting at 380 nm.

^c Electrochemical measurements were carried out in acetonitrile solution and the potentials are V vs. ferrocene/ferrocene ($\text{Fc}^{+/0}$).

^d Lifetime data are collected in degassed solutions.

^e Data taken from Ref. [24a].

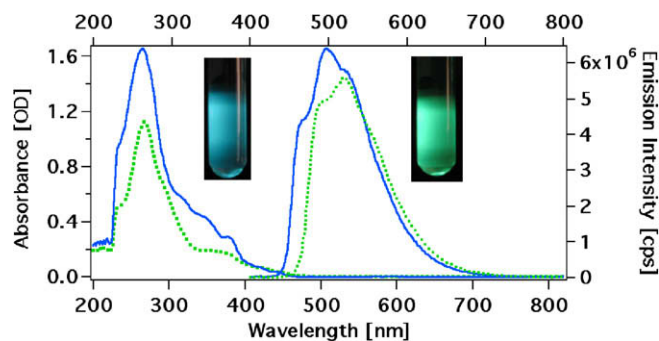


Fig. 4. Absorption and emission spectra of **40** (solid line) and **41** (dashed line) in dichloromethane solution at 298 K.

respectively (Table 7 and Fig. 4) [23]. When excited at 298 K within the π - π^* or MLCT absorption bands, complex **40** shows emission maxima at 463 and 493 nm due to the 4,4'-dimethylamino-2,2'-bipyridine ligand that increases the gap between LUMO of 4,4'-dimethylamino-2,2'-bipyridine and HOMO of Ir, resulting in a blue shift of the emission maxima compared to **39** [8,24a]. It is worth noting that the argon-degassed dichloromethane solutions of **40** and **41** show bright luminescence in a lighted room, and display unusual phosphorescence quantum yields of $80 \pm 10\%$ in solution at room temperature. Such result is of importance for unraveling the factors controlling the photoluminescence quantum yield of the complexes.

2.6. Controlling the phosphorescence quantum yield

Orthometallated iridium complexes are indeed known to have highest triplet emission quantum yields due to several factors [25]: (a) iridium has a large d-orbital splitting compared to other metals in the group; (b) strong ligand field strength of the ppy anionic ligand increases the d-orbital splitting, leading to an enlarged gap between the e_g orbitals of iridium and the LUMO of the ligand; (c) close-lying π - π^* and MLCT transitions, together with the heavy atom effect, enhance the spin-orbit coupling. However, the mixed ligand cationic Ir complexes show appreciably lower quantum yields compared to the tris-orthometallated Ir complexes because of the lower LUMO orbitals of the 2,2'-bipyridine ligand [8,24a,26]. One strategy to increase the quantum yields of Ir complexes is to introduce F and/or CF_3 substituents. This results in a stabilization of both the HOMO and the LUMO. Since the HOMO stabilization is larger than that of the LUMO, this leads to an increase in the HOMO-LUMO gap [27]. Another strategy, however, is to decrease the gap between the lowest π^* orbitals of the ppy ligand and the 2,2'-bipyridine ligand by introducing donor substituents such as dimethylamino groups at the 4,4'-positions of 2,2'-bipyridine that are known to have a strong destabilization effect on the LUMO* (see complexes **40** and **41**). In such type of complexes, the π - π^* and MLCT states associated with the ppy and 4,4'-dimethylamino-2,2'-bipyridine ligands are expected to be located closely

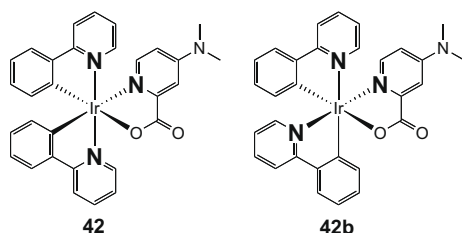


Fig. 5. Chemical structures of **42** and its isomer **42b**.

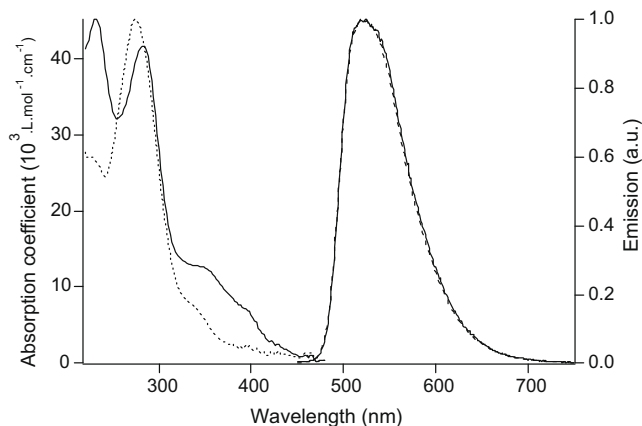


Fig. 6. Absorption and emission spectra in acetonitrile of **42** (dashed line) and **42b** (solid line).

together, which enhances the excited state decay through radiative pathways.

The quantum yields of Ir complexes can also be modulated by introducing ligands having strong ligand field stabilization energy, such as NCS^- and CN^- , as seen previously. In these complexes, the gap between the metal e_g and the ligand LUMO orbitals increases, resulting in a decay of the excited charge transfer states through radiative pathways [6d].

2.7. Sublimation not an innocent technique

Bis-cyclometallated iridium complexes have been always reported as having both neutral N-heterocycle (for example the pyridine in phenyl-pyridine based C[^]N ligand) in a *trans* position and the phenyl rings in a *cis*-position to each other. Very recently the first bis-cyclometallated iridium complex having the two pyridine fragments of the main cyclometallating ligand in a *cis*-position has been reported (Fig. 5) [28]. Emission spectra of **42** and **42b** are identical (Fig. 6) which is different from what is observed in the case of tris-cyclometallated complexes. Interestingly this isomer has been observed during the sublimation of the dopant during the preparation of vacuum processed OLED. This implies that when an iridium complex can be thermally isomerized, it would not be possible to prepare devices having a pure dopant, but rather a mixture of isomer as dopant. Such mixture may have a profound impact on the properties of the devices as it has been shown with tris-cyclometallated complexes, where *fac*-, and *mer*-complexes behave very differently in device. Characteristic of solution processed device containing pure **42** [29] and vacuum processed device containing a mixture of **42** and **42b** [28] are shown in Fig. 7. However, in this case, differences in devices architecture may be the main reason for observed differences (see references for details).

3. Iridium complexes for DSSC

Fig. 8 shows the operating principles of the dye-sensitized solar cell. The adsorbed sensitizer is excited by absorption of light, which leads to injection of electrons into the conduction band of the TiO_2 . The oxidized dye is subsequently reduced by electron donation from an electrolyte containing the iodide/triiodide redox system. The injected electron flows through the semiconductor network to arrive at the back contact and then through the external load to the counter electrode. At the counter electrode, reduction of triiodide in turn regenerates iodide, which completes the

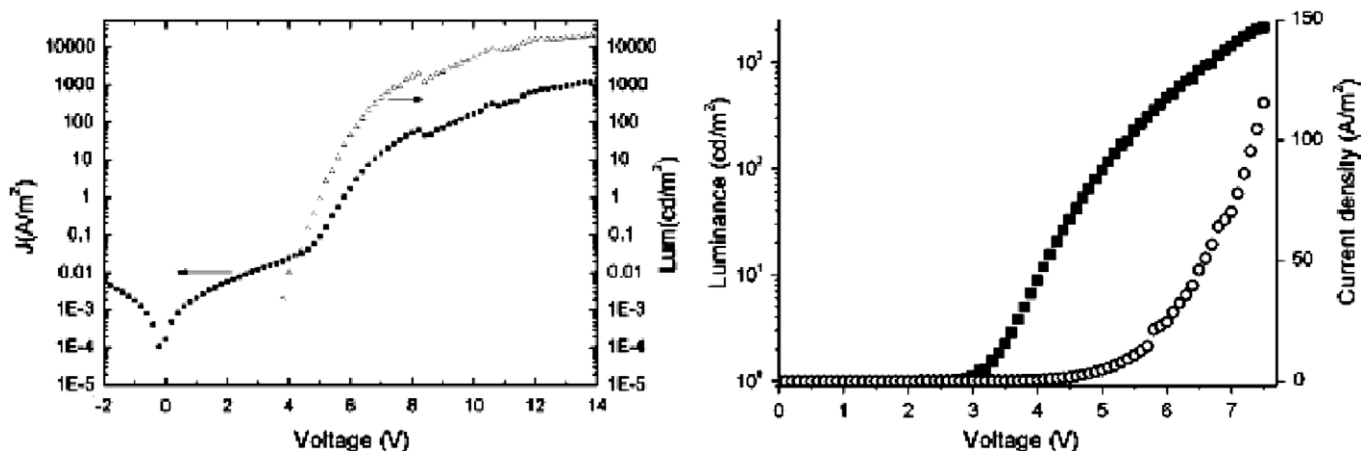


Fig. 7. Current density (solid squares) and luminance (open up triangles) vs. applied bias of the **42** containing solution processed OLED device (left panel). Luminance (solid squares) and current density (open circles) vs. applied bias of the **42**-based vacuum processed OLED device (right panel).

circuit. Under illumination, the device constitutes a regenerative and stable photovoltaic energy conversion system.

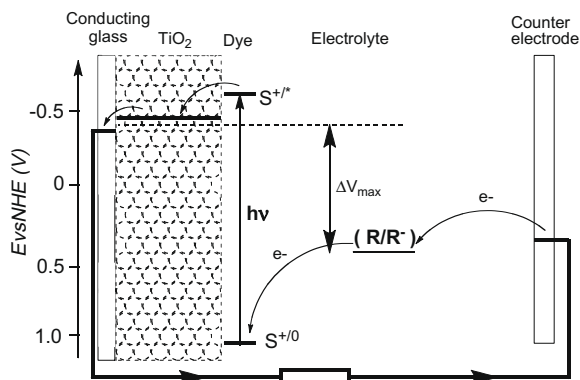


Fig. 8. Operating principles and energy level diagram of dye-sensitized solar cell. S^+/S^+ represent the sensitizer in the ground, oxidized, and excited state, respectively. R/R^- represents the redox mediator (I^-/I_3^-).

Some reactions are undesirable as resulting in losses in the cell efficiency. Those reactions are recombination of injected electrons either with oxidized sensitizer or with the oxidized redox couple at the TiO_2 surface. The surface of the nanocrystalline film is covered with a monolayer of the sensitizer S . The high surface area of the mesoporous metal oxide film is critical to efficient device performance as it allows strong absorption of solar irradiation to be achieved by only a monolayer of adsorbed sensitizer. The high surface area of such mesoporous films does however have a significant downside, as it also enhances interfacial charge recombination losses.

Ruthenium dyes are actually giving the most efficient devices. Efficiency is coming in a first approximation from the balance in the separation/recombination dynamics. The injection efficiencies are actually unity, and further improvement of devices could therefore come from a general strategy for reducing the recombination of charges. In this respect, dyes with injecting state having MLCT characters are very sensitive to the spatial separation with the electrode surface. An increase of this separation would decrease the back recombination but at the same time may be detrimental to the injection efficiency. LLCT are appealing as increased

Table 8
Structure of the dyes **43–45** and photoelectrochemical data of devices^a

Dye	J_{sc} ($mA\ cm^{-2}$)	V_{oc} (mV)	ff ^b	Eff ^c (%)	Φ^d (%)	E_{dark}^e (V)
43 [Ir(ppz) ₂ (dcbq)] ⁺	1.99	−380	0.66	0.5	60	−386
44 [Ir(ppz) ₂ (dcbpy)] ⁺	2.24	−438	0.67	0.65	100	−436
45 [Ru(bpy) ₂ (dcbpy)] ²⁺	3.35	−458	0.65	1.0	100	−476

^a Acetonitrile with 0.50 M LiI, 0.040 M I_2 , 20 mM pyridine, 20 mM pyridinium triflate under simulated AM 1.0 conditions.

^b The fill factor (ff).

^c The efficiency (Eff) is calculated as $(-J_{sc} V_{oc} ff\ 100\%)/I_s$, where $I_s = 100\ mW\ cm^{-2}$.

^d The integrated quantum yield (U) was determined by comparing the experimentally measured value of J_{sc} with the maximum calculated J_{sc} assuming a unity quantum yield when the measured absorbance of the dyes on TiO_2 electrodes were convoluted with the spectral irradiance of the solar simulator between 1100 and 360 nm.

^e Potential vs. the Nernst potential of the cell required to drive a cathodic current density of $-0.1\ mA\ cm^{-2}$ in the dark.

Table 9
Structure of the dyes **46–49** and photoelectrochemical data of devices.

Dye	J (mA cm ⁻²)	V (mV)	ff	Efficiency
46	0.27	457	0.75	0.09
47	2.70	500	0.69	0.94
48	2.70	408	0.72	0.79
49	4.30	590	0.74	1.87

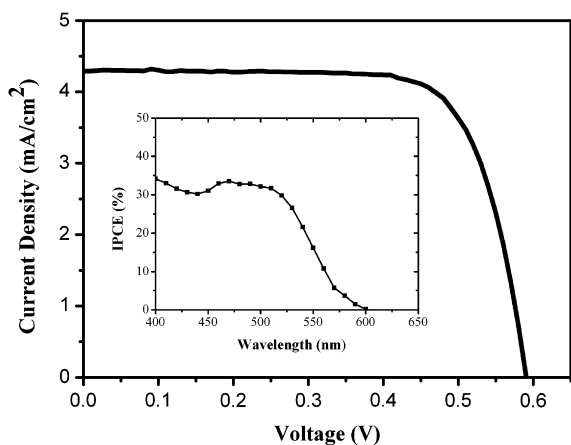


Fig. 9. I–V curve at full sun for DSSC using **49** as a dye. Inset shows the IPCE curve for the device.

separation distance may be obtained. To this end, cyclometallated iridium complexes have been investigated as sensitizers in TiO₂-based photoelectrochemical cells [5]. The two first iridium complexes reported for DSSC are shown in Table 8. LLCT transition from the cyclometallating phenylpyrazole (ppz) ligand to the dcbp (4,4'-dicarboxy-2,2'-bipyridine) or dcbq (4,4'-dicarboxy-2,2'-biquinoline) ligand was observed in the absorption spectra and confirmed by DFT calculations.

The iridium dye containing the 4,4'-dicarboxy-2,2'-bipyridine, **44**, is noteworthy as giving device with characteristic very close from the DSSC made using the ruthenium complex **43**, beside J_{sc} inducing a drop in efficiency. Despite poor characteristics of devices, iridium complexes may have some advantages compared to usual ruthenium complexes, like higher stability and less accessible MC states. In particular the authors think about the possibility engineering iridium complexes for dual sensitization, through LLCT and MLCT, which could improve the efficiency of the device.

Following the idea of increasing the separation distance, we prepared complex **46**, which contains a bipyridine ancillary ligand extended with carboxy-styrene moiety. J_{sc} is very low but V_{oc} is higher than with iridium complexes **44** and **45** (Table 9, unpublished data). Unexpectedly, when a simple dicarboxy-2,2'-bipyridine is used as ancillary ligand in complex **47**, the device characteristics increased dramatically and the efficiency is an order of magnitude higher compared to the complex **46**.

A modification of the phenyl-pyridine ligand like in complex **48**, leads to a drop of voltage, with no change of current. All those three complexes are expected to have a LUMO localized on the bipyridine ligand as seen previously in complexes for OLED application. When the attaching carboxy group is directly attached to the main ligand, as in complex **49**, the device characteristics are dramatically improved. The current–voltage characteristics and IPCE data for the complex **49** are shown in Fig. 9.

The main drawback in iridium sensitizers when compared to ruthenium sensitizers is that IPCE response, which does not extend beyond 600 nm in the former case where as in the latter case it extends close to 900 nm. Improving the absorption properties of iridium dye for DSSC is certainly a first point to focus on.

4. Future prospects

Cyclometallated iridium complexes are very efficient dopant for OLEDs applications. In two decades of research, deep understanding and large progress have been achieved in this respect and some devices reached in the market. However, challenge still remains in obtaining a stable white light-emitting device. Such goal will certainly be attained once a long-term stable dopant emitting blue light is designed. The main difficulty is on finding a relevant host for such wide gap material.

In the DSSC field, cyclometallated iridium complexes are just a nascent dye family. Large d-orbitals splitting leading to high MC states, likely to render the molecule more stable compared to ruthenium complexes, may be very advantageous for long-term stability issue. However, iridium complexes are not usually consid-

ered as strong absorbers, which is a key importance for device efficiency. By finding inspiration in the well known ruthenium dyes, it is however an exciting challenge to increase the molar extinction coefficient of iridium complexes to enhance light harvesting properties, which significantly improves the short-circuit current resulting in useful power conversion efficiencies.

Acknowledgements

We thank the Swiss Federal Office for Energy (OFEN) and the Solvay Centrale Recherche and Technologie Division for financial support.

References

- [1] (a) M.S. Lowry, S. Bernhard, *Chem. Eur. J.* 12 (2006) 7970;
(b) W.-Y. Wong, C.-L. Ho, *Coord. Chem. Rev.* doi:10.1016/j.ccr.2009.01.013;
(c) R.C. Evans, P. Douglas, C.J. Winscom, *Coord. Chem. Rev.* 250 (2006) 2093;
(d) P.-T. Chou, Y. Chi, *Chem. Eur. J.* 13 (2007) 380.
- [2] M.K. Nazeeruddin, F. De Angelis, S. Fantacci, A. Selloni, G. Viscardi, P. Liska, S. Ito, T. Bessho, M. Graetzel, *J. Am. Chem. Soc.* 127 (2005) 16835.
- [3] (a) M.K. Nazeeruddin, M. Graetzel, in: V. Ramamurthy, K.S. Schanze (Eds.), *Molecular and Supramolecular Photochemistry*, vol. 10, Marcel Dekker, New York, 2003, p. 301;
(b) M.K. Nazeeruddin, M. Graetzel, *Struct. Bond.* 123 (2007) 113.
- [4] (a) T. Bessho, E.C. Constable, M. Graetzel, A.H. Redondo, C.E. Housecroft, W. Klyberg, M.K. Nazeeruddin, M. Neuburger, S. Schaffner, *Chem. Commun.* (2008) 3717;
(b) D.P. Hagberg, J.H. Yum, H. Lee, F. De Angelis, T. Marinado, K.M. Karlsson, R. Humphry-Baker, L.C. Sun, A. Hagfeldt, M. Graetzel, M.K. Nazeeruddin, *J. Am. Chem. Soc.* 130 (2008) 6259;
(c) C. Kim, H. Choi, S. Kim, C. Baik, K. Song, M.S. Kang, S.O. Kang, J. Ko, *J. Org. Chem.* 73 (2008) 7072;
(d) K. Hara, T. Sato, R. Katoh, A. Furube, Y. Ohga, A. Shinpo, S. Suga, K. Sayama, H. Sugihara, H. Arakawa, *J. Phys. Chem. B* 107 (2003) 597;
(e) J.-J. Cid, J.-H. Yum, S.-R. Jang, M.K. Nazeeruddin, E. Martinez-Ferrero, E. Palomares, J. Ko, M. Grätzel, T. Torres, *Angew. Chem., Int. Ed.* 46 (2007) 8358.
- [5] E.I. Mayo, K. Kilsa, T. Tirrell, P.I. Djurovich, A. Tamayo, M.E. Thompson, N.S. Lewis, H.B. Gray, *Photochem. Photobiol. Sci.* 5 (2006) 871.
- [6] (a) C. Adachi, M.A. Baldo, M.E. Thompson, S.R. Forrest, *J. Appl. Phys.* 90 (2001) 5048;
(b) M.A. Baldo, S. Lamansky, P.E. Burrows, M.E. Thompson, S.R. Forrest, *Appl. Phys. Lett.* 75 (1999) 4;
(c) M. Ikai, S. Tokito, Y. Sakamoto, T. Suzuki, Y. Taga, *Appl. Phys. Lett.* 79 (2001) 156;
(d) M.K. Nazeeruddin, R. Humphry-Baker, D. Berner, S. Rivier, L. Zuppiroli, M. Graetzel, *J. Am. Chem. Soc.* 125 (2003) 8790.
- [7] (a) Y. Tao, Q. Wang, C. Yang, Q. Wang, Z. Zhang, T. Zou, J. Qin, D. Ma, *Angew. Chem., Int. Ed.* 47 (2008) 8104;
(b) S.-J. Su, T. Chiba, T. Takeda, J. Kido, *Adv. Mater.* 20 (2008) 2125.
- [8] K.A. King, R.J. Watts, *J. Am. Chem. Soc.* 109 (1987) 1589.
- [9] P.J. Hay, *J. Phys. Chem. A* 106 (2002) 1634.
- [10] (a) K. Dedeian, P.I. Djurovich, F.O. Garces, C. Carlson, R.J. Watts, *Inorg. Chem.* 30 (1991) 1685;
(b) S. Sprouse, K.A. King, P.J. Spellane, R.J. Watts, *J. Am. Chem. Soc.* 106 (1984) 6647.
- [11] C. Hansch, A. Leo, R.W. Taft, *Chem. Rev.* 91 (1991) 165.
- [12] (a) A. Tsuboyama, H. Iwawaki, M. Furugori, T. Mukaide, J. Kamatani, S. Igawa, T. Moriyama, S. Miura, T. Takiguchi, S. Okada, M. Hoshino, K. Ueno, *J. Am. Chem. Soc.* 125 (2003) 12971;
(b) G. Zhou, W.-Y. Wong, B. Yao, Z. Xie, L. Wang, *Angew. Chem., Int. Ed.* 46 (2007) 1149;
(c) C.-L. Ho, W.-Y. Wong, Z.-Q. Gao, C.-H. Chen, K.-W. Cheah, B. Yao, Z. Xie, Q. Wang, D. Ma, L. Wang, X.-M. Yu, H.-S. Kwok, Z. Lin, *Adv. Funct. Mater.* 18 (2008) 319.
- [13] B.M.J.S. Paulose, D.K. Rayabarapu, J.-P. Duan, C.-H. Cheng, *Adv. Mater.* 16 (2004) 2003.
- [14] T. Sajoto, P.I. Djurovich, A. Tamayo, M. Yousufuddin, R. Bau, M.E. Thompson, *Inorg. Chem.* 44 (2005) 7992.
- [15] S.J. Lee, K.-M. Park, K. Yang, Y. Kang, *Inorg. Chem.* 48 (2009) 1030.
- [16] A.B. Tamayo, B.D. Alleyne, P.I. Djurovich, S. Lamansky, I. Tsyba, N.N. Ho, R. Bau, M.E. Thompson, *J. Am. Chem. Soc.* 125 (2003) 7377.
- [17] R.J. Holmes, S.R. Forrest, T. Sajoto, A. Tamayo, P.I. Djurovich, M.E. Thompson, J. Brooks, Y.-J. Tung, B.W. D'Andrade, M.S. Weaver, R.C. Kwong, J.J. Brown, *Appl. Phys. Lett.* 87 (2005) 243507.
- [18] A.B. Tamayo, S. Garon, T. Sajoto, P.I. Djurovich, I.M. Tsyba, R. Bau, M.E. Thompson, *Inorg. Chem.* 44 (2005) 8723.
- [19] G. Zhou, C.-L. Ho, W.-Y. Wong, Q. Wang, D. Ma, L. Wang, Z. Lin, T.B. Marder, A. Beeby, *Adv. Funct. Mater.* 18 (2008) 499.
- [20] (a) P. Coppo, E.A. Plummer, L. De Cola, *Chem. Commun.* (2004) 1774;
(b) I. Avilov, P. Minoofar, J. Cornil, L. De Cola, *J. Am. Chem. Soc.* 129 (2007) 8247.
- [21] Y.-H. Song, Y.-C. Chiu, Y. Chi, Y.-M. Cheng, C.-H. Lai, P.-T. Chou, K.-T. Wong, M.-H. Tsai, C.-C. Wu, *Chem. Eur. J.* 14 (2008) 5423.
- [22] Y. You, S.Y. Park, *J. Am. Chem. Soc.* 127 (2005) 12438.
- [23] B. Schmid, F.O. Garces, R.J. Watts, *Inorg. Chem.* 33 (1994) 9.
- [24] (a) J.D. Slinker, A.A. Gorodetsky, M.S. Lowry, J. Wang, S. Parker, R. Rohl, S. Bernhard, G.G. Malliaras, *J. Am. Chem. Soc.* 126 (2004) 2763;
(b) M.K. Nazeeruddin, R.T. Wegh, Z. Zhou, C. Klein, Q. Wan, F. De Angelis, S. Fantacci, M. Grätzel, *Inorg. Chem.* 45 (2006) 9245;
(c) F. De Angelis, S. Fantacci, N. Evans, C. Klein, S.M. Zakeeruddin, J.-E. Moser, K. Kalyanasundaram, H.J. Bolink, M. Grätzel, M.K. Nazeeruddin, *Inorg. Chem.* 46 (2007) 5989.
- [25] (a) Y. Ohsawa, S. Sprouse, K.A. King, M.K. De Armond, K.W. Hanck, R.J. Watts, *J. Phys. Chem.* 91 (1987) 1047;
(b) F.O. Garces, K.A. King, R.J. Watts, *Inorg. Chem.* 27 (1988) 3464.
- [26] C.-H. Yang, S.-W. Li, Y. Chi, Y.-M. Cheng, Y.-S. Yeh, P.-T. Chou, G.-H. Lee, C.-H. Wang, C.-F. Shu, *Inorg. Chem.* 44 (2005) 7770.
- [27] M.S. Lowry, J.I. Goldsmith, J.D. Slinker, R. Rohl, R.A. Pascal, G.G. Malliaras, S. Bernhard, *Chem. Mater.* 17 (2005) 5712.
- [28] E. Baranoff, S. Suárez, P. Bugnon, C. Barolo, R. Buscaino, R. Scopelliti, L. Zuppiroli, M. Graetzel, M.K. Nazeeruddin, *Inorg. Chem.* 47 (2008) 6575.
- [29] H.J. Bolink, E. Coronado, S.G. Santamaria, M. Sessolo, N. Evans, C. Klein, E. Baranoff, K. Kalyanasundaram, M. Graetzel, M.K. Nazeeruddin, *Chem. Commun.* (2007) 3276.